

Evaluation of airborne TASI-600 imagery for mineral mapping of the Yerington skarn-porphyry system, Nevada

Background

Thermal infrared (TIR) wavelengths (7.5 to 14 μm) provide mineralogical information not available at the more commonly used/accessible visible to shortwave infrared (VNIR-SWIR) wavelengths (0.4 to 2.5 μm), including the content and physicochemical composition of feldspars, garnets, pyroxenes, olivines and silica minerals (e.g. quartz) as well as carbonates¹. A small number of TIR systems are now becoming operational, including: the drill core logging TIR-logger^{2,3}; satellite ASTER⁴ (five TIR bands); airborne SEBASS⁵ (128 bands); and airborne TASI-600⁶ (32 bands).

The specifications of the TASI-600 system (table below) are a useful analogue for future TIR satellite systems designed for enhanced global land surface composition mapping. To evaluate this potential, airborne TASI-600 imagery from the Yerington porphyry-skarn hydrothermal alteration system in Nevada^{7,8} were compared with ASTER and SEBASS data/products⁹. Key mineral products targeted include: (1) garnet Fe-Al composition; (2) carbonate Ca-Mg composition; (3) plagioclase Na-Ca composition; (4) clino-pyroxene (diopside); and (5) quartz. All of the remote sensing data were processed using a multi-parameter (feature depth/peak-height and wavelength position) plus masking approach¹⁰.

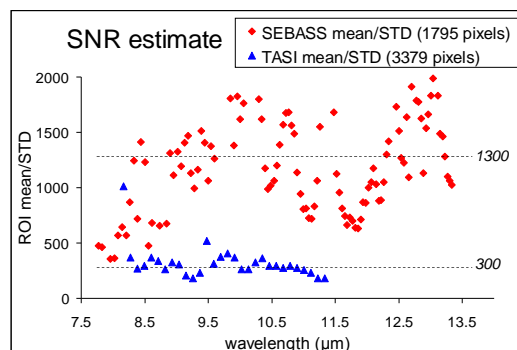
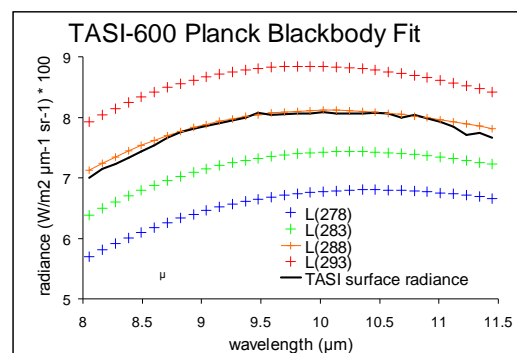
TASI-600 system and data

ITRES¹¹ (through Dr Stephen Achal) generously organised the collection and pre-processing (to geometrically-corrected mosaics of surface radiance) of the TASI-600 imagery from the Yerington test site (~6 by 6 km area) in August 2010.

The TASI-600 surface radiance spectra show characteristic Planck Blackbody behaviour as demonstrated by the pixel-spectrum of green vegetation (solid black line) which closely follows the modelled Planck function for 288°K. The small departures at either end of this spectral interval are similar to those observed for SEBASS data¹¹ and are interpreted to be residual errors related to the "In-Scene-Atmospheric-Correction" algorithm¹³, which does not account for atmospheric continuum-absorption or down-welling radiance.

The TASI-600 signal-to-noise (SNR) was estimated (mean/STD) and compared with SEBASS data collected from the same region of interest that comprised "spectral" materials and minimal variations in "brightness" temperature. The results show that the TASI-600 (blue triangles) has lower SNR compared with SEBASS (red diamonds) as expected given the major technical differences between these systems (SEBASS is liquid helium cooled whereas TASI is thermo-electrically cooled).

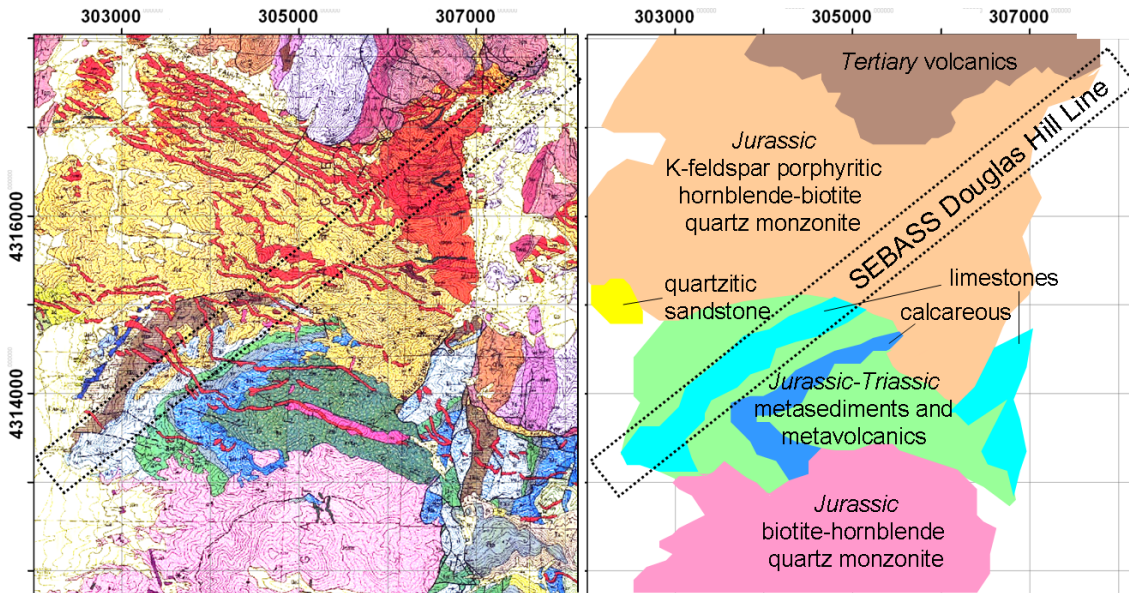
TASI-600	Specifications
area array (pushbroom)	600 pixels by 32 bands
spectral range	8 to 11.5 μm
NEΔT	0.2° at 300°K
IFOV / FOV	0.49 mRad / 40°
related sensors	CASI, SASI, MASI, TABI



Yerington Mineral Mapping

Geology

The published geology of the Yerington¹⁴ area comprises Jurassic-Triassic meta-volcanics and meta-sediments, including limestone (cyan), calcareous argillite (blue) and quartzitic sandstones (yellow) (figure below). These were intruded by Jurassic biotite-hornblende-quartz monzonites, both K-feldspar porphyritic (light brown – called the Yerington Batholith) and non-porphyritic (pink) types. The Yerington Batholith generated late-stage porphyry dykes and associated hydrothermal fluids which transported metals such as Cu. Miocene “Basin and Range” tectonics faulted/folded the rocks causing up to 80° westward tilt and related erosion before Tertiary volcanic rocks (brown) covered the sequence.

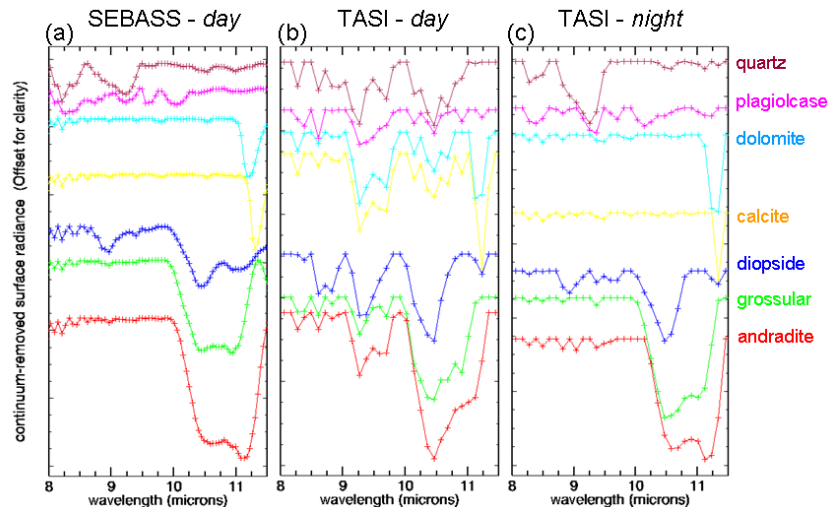


Spectral signatures

A selection of SEBASS and TASI-600 endmember spectra (next figure) of different mineral types show characteristic signatures in the TIR. However, the TASI-600 spectra from the day imagery are compromised by pronounced atmospheric residuals. The intensity of these systematic features is correlated with surface brightness temperature. As suggested above, this shows that an improved TIR atmospheric correction method is required. In addition, the spectral emissivity contrast (depth of reststrahlen minima) of the airborne TIR data is much less (<25%) compared with laboratory TIR emissivity (and reflectance) spectra of rocks and minerals¹². This is a function of the in-filling effects of down-welling sky radiance and can complicate the generation of seamless, accurate mineral maps.

The Fe-rich Ca-garnet andradite (red) shows longer wavelength

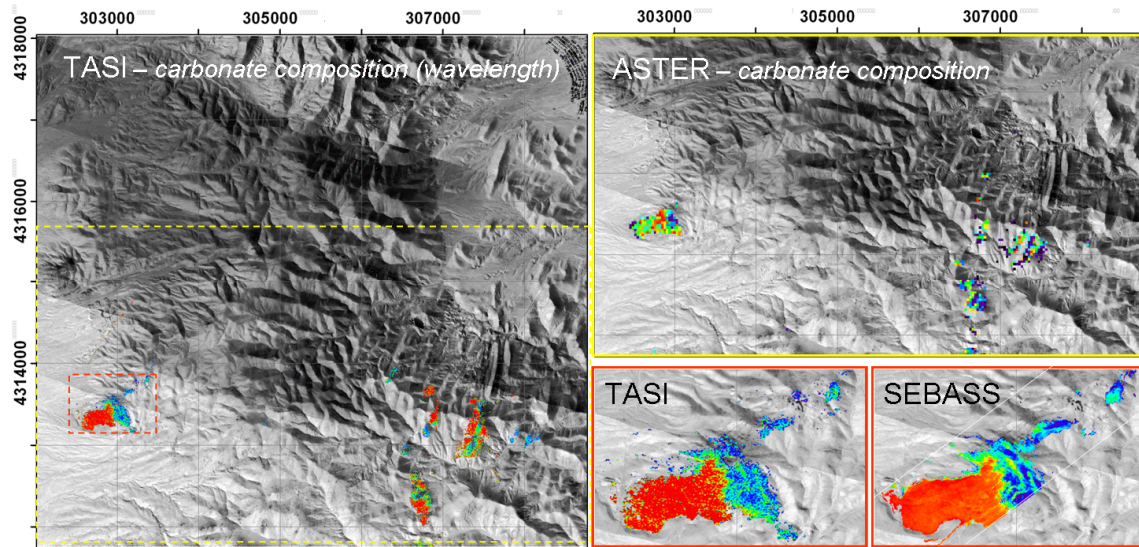
peaks and troughs compared with the Al-rich Ca-garnet, grossular (green). This is particularly evident in the SEBASS spectra though the TASI-600 spectra also show recognisable changes in wavelength near 11µm. The same is true for calcite (yellow) and dolomite (cyan). The diopside (blue) and plagioclase (magenta) spectra signatures are more difficult to recognise in the TASI-



600 spectra, especially for the diagnostic features in the 9-10 μm wavelength region, contrary to the SEBASS spectra.

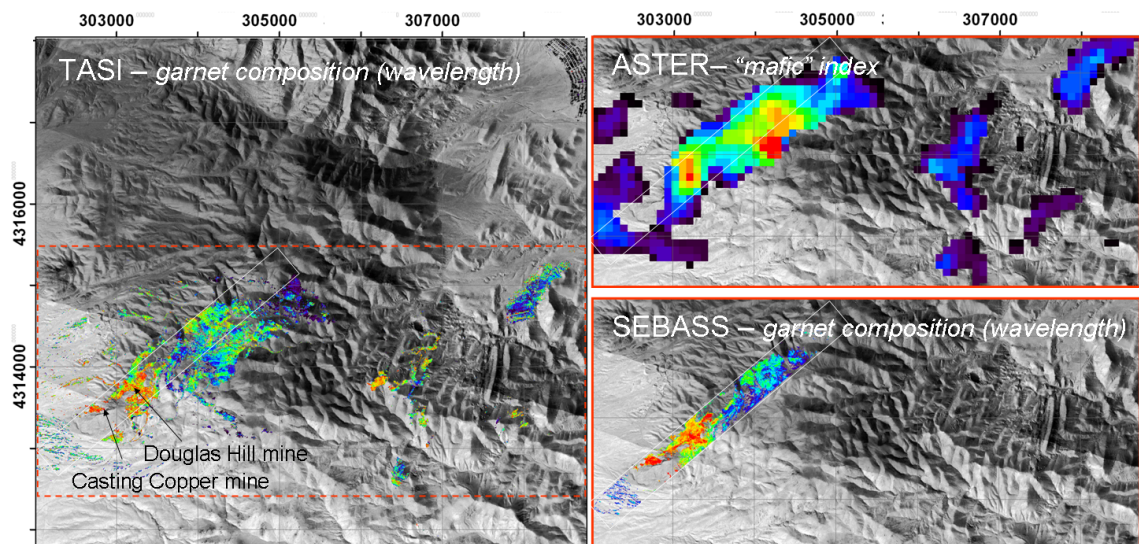
Carbonate mapping

The processed ASTER, SEBASS and TASI-600 data all show the same distribution of dolomite and calcite, albeit at different SNR levels. These include the southern part of the limestones covered by the Douglas Hill SEBASS run (see geology map above). In detail, SEBASS provides coherent mapping of carbonate mineralogy, including evident layering in dolomite (blue-cyan). In contrast, the TASI-600 results show weaker layering as well as a salt-and-pepper noise effect. Note that the ASTER carbonate map was generated using a combination of SWIR and TIR bands and that the entire study area was covered by the TASI-600 airborne survey (base-map is the day-time mosaic of TASI-600 surface radiance at 9.478 μm).



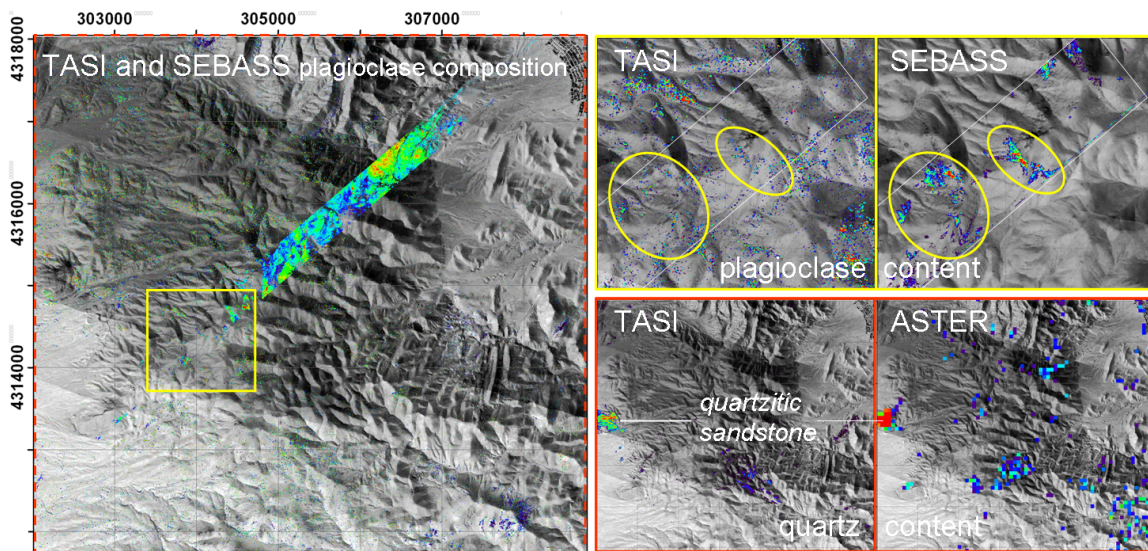
Garnet mapping

The carbonate-rich rocks were in large part altered to skarns that comprise minerals like garnet and diopside. All the processed ASTER, SEBASS and TASI-600 data reveal the wide extent of this skarn alteration, including within metavolcanics not mapped previously as calcareous (see the geology map). However, only SEBASS and TASI-600 afford the tracking of the wavelength (composition) of the garnets from Fe-rich andradite (red) to Al-rich grossular (blue). Importantly, there is high correspondence between these systems/maps. From an exploration perspective, high-grade Cu deposits, such as the Casting Copper and Douglas Hill deposits (labelled), are located where andradite is developed in close proximity to dolomite¹⁵.



Plagioclase and quartz mapping

SEBASS is useful for measuring/mapping the very small diagnostic features associated with feldspar minerals^{12,15}. This is shown by the extensive areas of plagioclase mapped in the monzonite (next figure) ranging from Na-rich albite (blue) to more Ca-rich oligoclase (yellow-red). However this information is not well reproduced using the TASI-600 data which appears to be nearing its SNR limit evident by extensive random noise. In detail (yellow boxes), the depth (~content) of the plagioclase 9.6 μm reststrahlen minimum shows this noise related salt-and-pepper effect. However, some more coherent areas (e.g. yellow ellipses that are associated with porphyry dykes) are weakly consistent with the SEBASS results.



Similar noise related issues were also noted for the diopside product that incorporated the use of 9.0 μm (as well as other) feature. Finally, mapping quartz (red boxes), including the quartzitic sandstones (see geology figure), is relatively easy with all three TIR systems.

Conclusion

The airborne TASI-600 sensor is well calibrated and of sufficiently high spectral and radiometric resolution to enable the measurement and mapping of a range of TIR-active minerals, including the contents and chemistry of carbonate (calcite and dolomite), garnet (Fe-rich andradite to Al-rich grossular), quartz and to a lesser degree, clino-pyroxene (diopside) and plagioclase (content only). There are many other minerals in the Yerington study area that can be mapped using the TASI-600 (e.g. epidote, kaolinite, gypsum), though these can also be mapped at VNIR-SWIR wavelengths. The TIR data also reveal many other spectral signatures related to plant and urban materials that may be of value for other applications. Combined, the results show the value of TASI-600 type specifications for future satellite TIR sensors.

References:

1. Lyon and Burns 1963. *Economic Geology*, 58, pp. 274-284.
2. www.csiro.au/science/hylogging-systems--ci_pageNo-3.html
3. Cudahy *et al.* 2009. *Economic Geology*, 16, 223-235.
4. Abrams *et al.* 2002. *JPL Publication*, 2, 25.
5. Hackwell *et al.* 1996. *SPIE* Vol. 2819, pp. 102-107
6. <http://www.itres.com/assets/pdf/TASI-600.pdf>
7. Dilles *et al.* 2000. *Economic Geology*, Guidebook Series Vol. 32, pp. 55-66
8. Einaudi 1977. *Economic Geology*, Vol. 72, pp. 769-795.
9. ftp://ftp.arcc.csiro.au/NGMM/Thermal_Reports
10. <http://c3dmm.csiro.au/kalgoorlie/kalgoorlie.html>
11. <http://www.itres.com>
12. Cudahy *et al.*, 2000. CSIRO Earth Science and Resource Engineering Report No 734R.
13. Johnson 1998. Aerospace Report No. ATR-99(8407)-1 Pt I.
14. Proffett and Dilles 1984. Nevada Bureau of Mines and Geology, Map 77, 89557-0088.
15. Cudahy *et al.*, 2000. CSIRO Earth Science and Resource Engineering Report No 1121R.

CSIRO Earth Science and Resource Engineering

Contact Dr Tom Cudahy Mobile 61-407-662-369
Phone 618-6436-8630 Email thomas.cudahy@csiro.au

Webpage <http://c3dmm.csiro>



WA Centre of Excellence
3D Mineral Mapping